STRUCTURAL CHEMISTRY

ISSN: 2053-2296
journals.iucr.org/c

# Structural and theoretical characterization of a new twisted 4′-substituted terpyridine compound: 4′-(isoquinolin-4-yl)-2,2′:6′,2″-terpyridine

**Juan Granifo, Beatriz Arévalo, Rubén Gaviño, Sebastián Suárez and Ricardo Baggio**

*Acta Cryst.* (2016). C**72**, 932–938

Acta Cryst C STRUCTURAL CHEMISTRY
ISSN 2053-2296

# Structural and theoretical characterization of a new twisted 4′-substituted terpyridine compound: 4′-(isoquinolin-4-yl)-2,2′:6′,2″-terpyridine

Juan Granifo,[a]‡ Beatriz Arévalo,[a] Rubén Gaviño,[b] Sebastián Suárez[c,d] and Ricardo Baggio[d]*§

[a]Departamento de Ciencias Químicas y Recursos Naturales, Facultad de Ingeniería y Ciencias, Universidad de La Frontera, Casilla 54-D, Temuco, Chile, [b]Instituto de Química, Universidad Nacional Autónoma de México, Cd. Universitaria, Circuito Exterior Coyoacán, 04510 México, México, [c]Departamento de Química Inorgánica, Analítica y Química, Física/INQUIMAE–CONICET, Facultad de Ciencias Exactas y Naturales, Universidad de Buenos Aires, Buenos Aires, Argentina, and [d]Gerencia de Investigación y Aplicaciones, Centro Atómico Constituyentes, Comisión Nacional de Energía Atómica, Buenos Aires, Argentina. *Correspondence e-mail: seba@qi.fcen.uba.ar

Received 21 September 2016
Accepted 17 October 2016

Edited by J. White, The University of Melbourne, Australia

‡ Author to whom enquires should be addressed, at juan.granifo@ufrontera.cl.
§ Author to whom enquires should be addressed, at baggio@cnea.gov.ar.

**Keywords:** atoms-in-molecules; AIM; 4′-substituted 2,2′:6′,2″-terpyridine; attractive H···H interaction; crystal structure; Bader's theory; theoretical characterization.

**CCDC reference**: 1510131

**Supporting information**: this article has supporting information at journals.iucr.org/c

4′-Substituted derivatives of 2,2′:6′,2″-terpyridine with N-containing heteroaromatic substituents, such as pyridyl groups, might be able to coordinate metal centres through the extra N-donor atom, in addition to the chelating terpyridine N atoms. The incorporation of these peripheral N-donor sites would also allow for the diversification of the types of noncovalent interactions present, such as hydrogen bonding and $\pi$–$\pi$ stacking. The title compound, $C_{24}H_{16}N_4$, consists of a 2,2′:6′,2″-terpyridine nucleus (tpy), with a pendant isoquinoline group (isq) bound at the central pyridine (py) ring. The tpy nucleus deviates slightly from planarity, with interplanar angles between the lateral and central py rings in the range 2.24 (7)–7.90 (7)°, while the isq group is rotated significantly [by 46.57 (6)°] out of this planar scheme, associated with a short $H_{tpy}\cdots H_{isq}$ contact of 2.32 Å. There are no strong noncovalent interactions in the structure, the main ones being of the $\pi$–$\pi$ and C—H$\cdots\pi$ types, giving rise to columnar arrays along [001], further linked by C—H$\cdots$N hydrogen bonds into a three-dimensional supramolecular structure. An Atoms In Molecules (AIM) analysis of the noncovalent interactions provided illuminating results, and while confirming the bonding character for all those interactions unquestionable from a geometrical point of view, it also provided answers for some cases where geometric parameters are not informative, in particular, the short $H_{tpy}\cdots H_{isq}$ contact of 2.32 Å to which AIM ascribed an attractive character.

## 1. Introduction

4′-Substituted derivatives of the tridentate 2,2′:6′,2″-terpyridine ligand have been synthesized in the past with the aim of providing the molecules with novel properties (Constable, 2007; Eryazici *et al.*, 2008). For example, those with N-containing heteroaromatic substituents, such as pyridyl groups, might be able to coordinate metals centres in addition to the chelating terpyridine N atoms. Furthermore, the incorporation of these peripheral N-donor sites would allow for the diversification of the types of noncovalent interactions present, such as hydrogen bonding, $\pi$–$\pi$ stacking, *etc*. Since, to the best of our knowledge, crystal structures of free 2,2′:6′,2″-terpyridines 4′-functionalized with N-containing fused-ring systems have not been reported, we focused this study on the molecular structure and supramolecular properties of a derivative with an isoquinolin-4-yl moiety [see (I) in the Scheme]. So far, X-ray diffraction studies of only two structures with polyaromatic fused-ring systems as substituents in 4′-functionalized

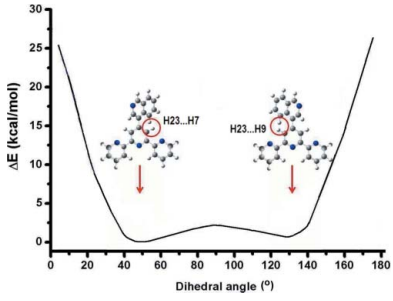

2,2′:6′,2″-terpyridines have been reported (Gulyani *et al.*, 2002), *viz.* 4′-(anthracen-9-yl)-2,2′:6′,2″-terpyridine, (II), and 4′-(pyren-1-yl)-2,2′:6′,2″-terpyridine, (III) (see Scheme). Both structures are twisted, with dihedral angles between the fused-ring planes (anthracen-9-yl and pyren-1-yl) and the central pyridine (py) of the terpyridine fragment of 74.5 (2) and 51.6 (2)°, respectively. A plausible explanation for these torsions with respect to a planar conformation was provided by considering that in this conformation the repulsive interaction between H atoms in the central pyridyl ring and those in the fused-ring system are minimized. Herein, we present the crystal structure of 4′-(isoquinolin-4-yl)-2,2′:6′,2″-terpyridine, (I), which is also twisted and shows a set of noncovalent $\pi$–$\pi$, C—H···$\pi$ and C—H···N interactions, all of which are discussed in the light of Bader's theory of Atoms In Molecules (AIM).

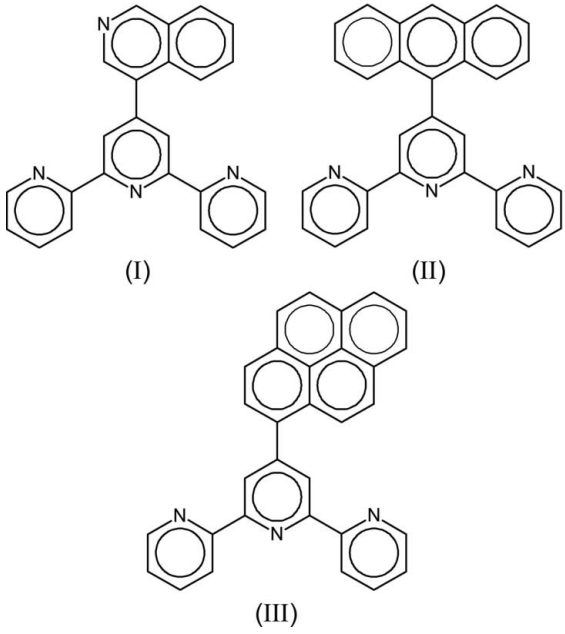


## 2. Experimental

The solvents were purchased from commercial sources and were used without further purification. IR spectra were recorded on a Bruker Tensor 27 FT–IR spectrometer (using KBr plates) or an Agilent Cary 630 FT–IR spectrometer using a Diamond ATR accessory. An Exeter Analytical CE-440 elemental analyzer was used for microanalyses (C, H and N). $^1$H and $^{13}$C NMR spectra were recorded on a Bruker Advance 300 MHz spectrometer, with the chemical shifts referenced to TMS. Electrospray ionization (ESI) mass spectra were measured on a Bruker Esquire 6000. X-ray diffraction data were collected with an Oxford Diffraction Xcalibur CCD Eos Gemini diffractometer with graphite-monochromatized Mo $K\alpha$ radiation.

### 2.1. Synthesis and crystallization

4′-(Isoquinolin-4-yl)-2,2′:6′,2″-terpyridine was prepared using the one-pot method of Hanan & Wang (2005). 2-Acetylpyridine (0.61 g 5.0 mmol) was added to a solution of isoquinoline-4-carbaldehyde (0.40 g, 2.5 mmol) in EtOH (20 ml) and the mixture was stirred for 15 min. KOH pellets (0.30 g, 5.4 mmol) and an excess of aqueous $NH_3$ (8.0 ml, 25%, 107 mmol) were added. The resulting solution was stirred at room temperature for a period of 15 h. The light-brown precipitate which formed was filtered off and washed with water (4 × 10 ml). The product was dissolved in $CH_2Cl_2$ (20 ml) and then methanol (15 ml) was added. The solution was refrigerated overnight to give well-formed colourless crystals, which were washed with methanol (2 × 5 ml) (yield 0.14 g, 15%). ESI–MS (MeOH): $m/z$ 361.1 $[M + H]^+$ (calculated 361.1). Analysis calculated for $C_{24}H_{16}N_4$: C 79.98, H 4.47, N 15.55%; found: C 79.94, H 4.45, N 15.48%. ATR FT–IR (cm$^{-1}$): 3090 (*w*), 3049 (*w*), 3011 (*w*), 1584 (*s*), 1566 (*s*), 1543 (*s*), 1500 (*w*), 1487 (*s*), 1415 (*m*), 1386 (*s*), 1268 (*m*), 1218 (*w*), 117 (*m*), 1096 (*w*), 1089 (*m*), 1022 (*w*), 989 (*m*), 895 (*m*), 887 (*m*), 795 (*s*), 749 (*s*), 685 (*m*), 665 (*m*), 631 (*s*). $^{13}$C-PND and $^{13}$C-DEPT NMR (75 MHz, $CDCl_3$, 298 K): $\delta$ 155.9 ($C_{quat}$, C13/C15), 155.8 ($C_{quat}$, C17/C17′), 152.9 (CH, C1), 149.2 (CH, C19/C19′), 147.1 ($C_{quat}$, C11), 142.5 (CH, C3), 136.9 (CH, C21/C21′), 133.6 ($C_{quat}$, C10), 131.3 ($C_{quat}$, C4), 131.1 (CH, C6), 128.2 ($C_{quat}$, C9), 128.0 (CH, C8), 127.4 (CH, C7), 124.4 (CH, C5), 123.9 (CH, C22/C22′), 122.2 (CH, C12/C16), 121.3 (CH, C20/C20′). $^1$H NMR (300 MHz, $CDCl_3$, 298 K): $\delta$ 9.33 (*d*, 1H, $J$ = 0.9 Hz, H1), 8.72 (*t*, 2H, $J$ = 0.9, 8.1 Hz, H19/H19′), 8.68 (*ddd*, 2H, $J$ = 0.9, 1.8, 4.8 Hz, H22/H22′), 8.66 (*s*, 2H, H12/H16), 8.64 (*s*, 1H, H3), 8.08 (*m*, 1H, H8), 7.98 (*m*, 1H, H5), 7.90 (*ddd*, 2H, $J$ = 1.8, 7.5, 8.1 Hz, H21/

**Table 1**
Experimental details.

| | |
|---|---|
| Crystal data | |
| Chemical formula | $C_{24}H_{16}N_4$ |
| $M_r$ | 360.41 |
| Crystal system, space group | Monoclinic, $P2_1/n$ |
| Temperature (K) | 170 |
| $a$, $b$, $c$ (Å) | 12.3897 (3), 8.7940 (3), 17.1791 (6) |
| $\beta$ (°) | 108.369 (3) |
| $V$ (Å$^3$) | 1776.38 (10) |
| $Z$ | 4 |
| Radiation type | Mo $K\alpha$ |
| $\mu$ (mm$^{-1}$) | 0.08 |
| Crystal size (mm) | 0.34 × 0.22 × 0.12 |
| Data collection | |
| Diffractometer | Oxford Diffraction Xcalibur CCD (Eos, Gemini) |
| Absorption correction | Multi-scan (*CrysAlis PRO*; Oxford Diffraction, 2009) |
| $T_{min}$, $T_{max}$ | 0.97, 1.00 |
| No. of measured, independent and observed [$I > 2\sigma(I)$] reflections | 18351, 4225, 3138 |
| $R_{int}$ | 0.038 |
| (sin $\theta/\lambda)_{max}$ (Å$^{-1}$) | 0.681 |
| Refinement | |
| $R[F^2 > 2\sigma(F^2)]$, $wR(F^2)$, $S$ | 0.044, 0.123, 1.02 |
| No. of reflections | 4225 |
| No. of parameters | 254 |
| H-atom treatment | H-atom parameters constrained |
| $\Delta\rho_{max}$, $\Delta\rho_{min}$ (e Å$^{-3}$) | 0.26, −0.20 |

Computer programs: *CrysAlis PRO* (Oxford Diffraction, 2009), *SHELXS97* (Sheldrick, 2008), *SHELXTL* (Sheldrick, 2008), *Mercury* (Macrae *et al.*, 2006), *SHELXL2014* (Sheldrick, 2015) and *PLATON* (Spek, 2009).

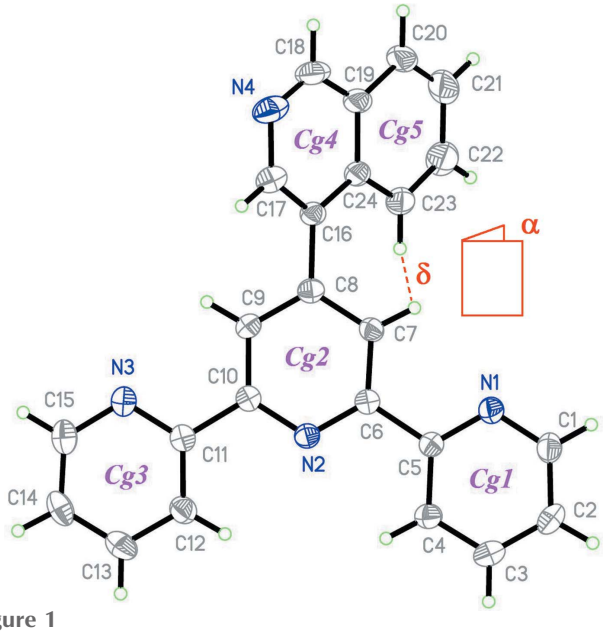


**Figure 1**
The molecular structure of (I), with displacement ellipsoids drawn at the 50% probability level. The H···H contact and torsion angle discussed in the text are indicated in red.

21′), 7.71 (*m*, 1H, H6), 7.66 (*m*, 1H, H7), 7.35 (*ddd*, 2H, $J$ = 1.2, 4.8, 7.5 Hz, H20/H20′).

### 2.2. Refinement

Crystal data, data collection and structure refinement details are summarized in Table 1. All H atoms were identified in an intermediate difference map, further idealized and finally refined as riding (C—H = 0.93 Å), with displacement parameters taken as $U_{iso}$(H) = 1.2$U_{eq}$(C).

### 2.3. Molecular calculations

Quantum-mechanical calculations were performed at the PBEPBE-D-6311++G(d,p) level of theory using the crystallographic coordinates (single-point calculations) within the *GAUSSIAN09* program (Frisch *et al.*, 2009), with C—H distances normalized to 'neutron values' (1.08 Å). The basis set superposition error for the calculation of interaction energies was corrected using the counterpoise method. The AIM analysis of the electron density was performed at the same level of theory using the *Multiwfn* program (Lu & Chen, 2012).

## 3. Results and discussion

### 3.1. Nuclear magnetic resonance

The NMR spectra of (I) in $CDCl_3$ solution [assigned through $^1$H–$^1$H Correlation Spectroscopy (COSY), Proton Noise Decoupled (PND), Distortionless Enhancement by Polarization Transfer (DEPT), Heteronuclear single-quantum correlation spectroscopy (HSQC) and Heteronuclear multiple-bond correlation spectroscopy (HMBC)] were in good agreement with the expected molecular structure (see Figs. S1, S2 and S3 in the *Supporting information*). Thus, analysis of the $^1$H (Fig. S1) and $^{13}$C NMR (Fig. S2) spectra indicated the presence of a monosubstituted isoquinolin-4-yl ring, a 2,4,6-trisubstituted pyridinyl ring and two 2-substituted pyridinyl rings. It should be noted that the $^1$H signal at 9.33 ppm assigned to atom H1 appeared as a doublet, due to the five-bonds-coupling between atoms H1 and H5 in the isoquinoline ring. Besides, the $^{13}$C NMR spectrum showed 17 signals, which were categorized by DEPT as 11 methine and six nonprotonated C atoms (Fig. S3).

### 3.2. X-ray diffraction

The crystal and molecular structure of (I) was determined by single-crystal X-ray diffraction at 170 (2) K. Relevant experimental data is presented in Table 1 and Fig. 1 shows the molecular geometry, as well as the atom and ring labelling. The bond lengths and angles are unremarkable. The molecule consists of a 2,2′-terpyridine nucleus (tpy), with the lateral pyridyl (py) rings having their N atoms (N1 and N3) *trans* to that (N2) of the central py ring [torsion angles N1—C5—C6—N2 = 172.22 (12)° and N2—C10—C11—N3 = 178.79 (11)°]. This is the usual disposition in free 2,2′-tpy groups, but contrasts with the configuration adopted when the molecule acts as a ligand, in its usual tridentate mode, where the lateral rings are rotated by 180° in order to enable triple coordination to a single cation (*e.g.* Constable, 2007; Eryazici *et al.*, 2008). It could be argued, at first sight, that the disposition adopted in (I) might favour the formation of four different weak intramolecular C—H···N contacts [H7···N1 = 2.483 (2) Å, H4···N2 = 2.514 (2) Å, H12···N2 = 2.473 (2) Å and H9···N3 = 2.507 (2) Å], possibly stabilizing the structure, but in fact, these N···H distances and C—H···N angles lie in the acceptability borderline for this type of intramolecular interaction, leaving the question open to further clarification (see below). The molecule is completed by a pendant isoquinoline

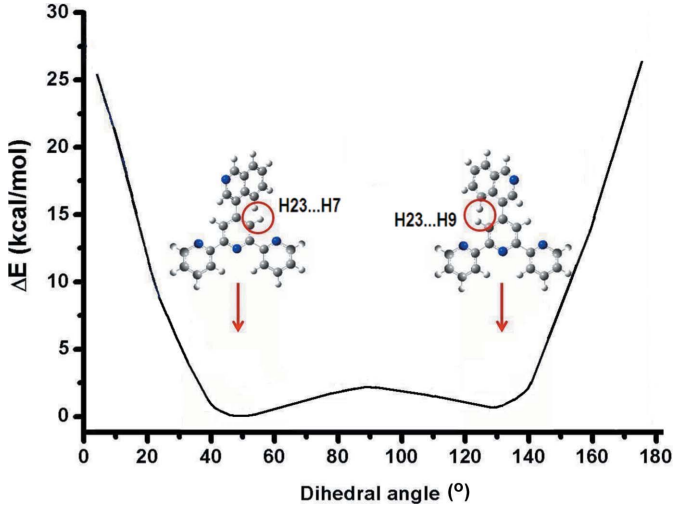


**Figure 2**
A schematic representation of the quasi-symmetrical rotational energy barrier as a function of the rotation of the isoquinoline group. The slight deviations from specular symmetry are apparent.

(isq) group bound to the central py ring. The tpy nucleus departs slightly from planarity (the interplanar angles between the py rings are given in Table 2), but the isq group, instead, is rotated significantly by 46.57 (6)° out of this planar scheme. This is the forced result of steric hindrance, needed to minimize 'bumping' between atoms H7 and H23. In our refined model with C—H = 0.96 Å, the intramolecular H7···H23 distance is 2.32 Å, while in a hypothetical planar disposition, this distance would collapse down to ≃0.80 Å. This argument appears to be reinforced by the difference between the angles centred at atom C16 [C24—C16—C8 = 122.72 (12)° and C17—C16—C8 = 119.12 (13)°], suggesting an H7···H23 repulsion. Fig. 2 presents a schematic representation of the energy barrier representing this steric hindrance; it shows a plot of the total energy calculated (for the X-ray model) as a function of the rotation angle around the C16—C8 bond linking tpy and isq, plotted in the 0–180° range. The diagram shows two extremely large maxima at 0 and 180° (corresponding to the tpy + isq 'planar' geometries), at both sides of which the curve is similar (in fact, symmetrical for a strictly planar tpy). There are, in addition, two local maxima at 90 and 270°, around which the curve would also be symmetrical, in which case the 'pivotal axis' C16—C8 is an exact bisector of the tpy group. In the present case, both conditions are slightly violated, and the concomitantly small departures from true symmetry can be observed in Fig. 2. Incidentally, since $P2_1/n$ includes symmetry operations of the first and the second kind, symmetry-related rotational conformers (see *A* and *B* in Fig. 4) co-exist in the crystal structure.

In this context, the short H7···H23 ≃ 2.32 Å distance should be *prima facie* ascribed an 'antibonding' character. Associated with this short H···H distance, the interplanar angle in (I) leans toward 'smaller-than-average' values in the wide distribution which is typical for quinoline derivatives joined to phenyl rings [including those described in Gulyani *et al.* (2002)]. Fig. 3 shows histograms of dihedral angle and the corresponding H···H distances as found in ≃1100 such structures in the Cambridge Structural Database (CSD, Version 5.37; Groom *et al.*, 2016; search target as in Fig. 3 inset). The results suggest that the 46.57 (6)°/2.32 Å pair in (I) falls in a rather low-angle short-contact region, something we shall also discuss below.

As expected from the outset (due to the lack of strong hydrogen-bonding donors), there are no strong packing interactions in the crystal structure. The few relevant interactions are presented in Table 3 (C—H···N and C—H···$\pi$) and Table 4 ($\pi$-stacking). The first column in these tables includes a sequence number, for convenience of description, and the last two columns include relevant parameters from AIM calculations. The packing building blocks are the columnar structures shown in Fig. 4(*a*), internally connected through $\pi$–$\pi$ interactions (#3 and #4 in Table 4), which generate dimeric units including both rotational conformers (*A* and *B*) built up around two types of inversion centres alternating at ($\frac{1}{2}$, 0, 0) and ($\frac{1}{2}$, $\frac{1}{2}$, 0). These columns, in turn, interact with those generated by the $2_1$ axis through the almost colinear C—H···$\pi$ (#2 in Table 3) and $\pi$–$\pi$ (#5 in Table 4)

**Table 2**
Relevant dihedral angles (°) between aromatic rings.

The ring codes are as in Fig. 1 and isq is isoquinoline.

| | |
|---|---|
| *Cg*2···*Cg*1 | 7.90 (7) |
| *Cg*2···*Cg*3 | 2.24 (7) |
| *Cg*4···*Cg*5 | 1.91 (8) |
| *Cg*2···isq | 46.57 (6) |

contacts running roughly along [301] to make broad two-dimensional structures parallel to ($\bar{1}$03). The latter are further linked through different C—H···N hydrogen bonds (#1 and #1* in Table 3) along [$\bar{1}$01]. In this way, a weakly bound three-dimensional supramolecular structure builds up (Fig. 4*b*).

### 3.3. AIM results

At this stage, a number of unanswered questions have been posed regarding possible (even if doubtful) noncovalent interactions for which the simple geometrical arguments at hand cannot provide adequate answers. This prompted us to go a bit further into the analysis, through an investigation of the electron-density topology *via* the AIM (an acronym for the 'Atoms In Molecules' theory; Bader, 1990) theoretical framework. The idea was to assess possible assignment to these interactions with some degree of confidence. AIM interprets chemical bonding in terms of shared (covalent bonds) or closed-shell (hydrogen bonding, ionic bonding, van der Waals, *etc.*) interactions. The relevant parameters used to characterize the attractive bonding character of short contacts are the electron density [$\rho(r)$], its gradient vector [$\nabla\rho(r)$], its Laplacian [$\nabla^2\rho(r)$], and the kinetic, potential and total energy densities in the region of the 'Bond Critical Point' (BCP) [$G(r)$, $V(r)$ and $E(r)$].

In some seminal papers on the subject (Bader, 1990, 2009), the author discloses two fundamental concepts on which the theory is based, *viz.* the 'Bonding Path' (BP), a line linking atomic nuclei along which the charge density has a maximum with respect to any lateral shift, and the BCP, an eventual minimum along these lines which provides an indicator of interatomic interaction. In addition, the sign and magnitude of $\rho(r)$ and $\nabla^2\rho(r)$ at the BCP characterizes the interaction type. The interactions are considered as 'shared' when $\nabla^2\rho(r) < 0$ (*viz.* electronic charge is concentrated at the BCP) or of the 'closed-shell' type when $\nabla^2\rho(r) > 0$ (*viz.* electronic charge drifts away from the interatomic surface towards the nuclei). In this latter case, $\rho(r)$ is relatively low in value.

Before going any further it must be stressed that AIM has been a matter of debate on theoretical grounds [*viz.* Haaland *et al.* (2004), Poater *et al.* (2006), and Krapp & Frenking (2007) *versus* Bader (2009)] and continues to be a controversial issue [Dunitz (2015) *versus* Thakur *et al.* (2015), and Lecomte *et al.* (2015)]. Even if now accepted as an extremely valuable tool, some critical viewpoints concerning the application of the method when 'absolute' AIM values are analyzed have been raised (Spackman, 2015); nevertheless, its use for 'relative' comparisons (as in the present approach) is steadily gaining general acceptability (Wang *et al.*, 2016, *etc.*)

**Table 3**
Hydrogen-bond geometry.

The ring codes are defined in Fig. 1.

| Interaction code | $D$—H···$A$ | $D$—H (Å) | H···$A$ (Å) | $D$···$A$ (Å) | $D$—H···$A$ (°) | $100\rho(r)$ (a.u) | $100\nabla^2\rho(r)$ (a.u) |
|---|---|---|---|---|---|---|---|
| #1 | C3—H3···N4$^{i}$ | 0.93 | 2.54 | 3.389 (2) | 152 | 1.26 | 0.36 |
| #1* | C13—H13···N1$^{ii}$ | 0.93 | 2.73 | 3.441 (2) | 134 | 0.80 | 0.24 |
| #2 | C15—H15···$Cg5^{ii}$ | 0.93 | 2.97 | 3.665 (2) | 132 | 0.48 | 0.13 |

Symmetry codes: (i) $x+\frac{1}{2}, -y+\frac{1}{2}, z-\frac{1}{2}$; (ii) $x-\frac{1}{2}, -y+\frac{1}{2}, z-\frac{1}{2}$.

When applied to our refined model, with C—H distances normalized to 'neutron' values (C—H = 1.08 Å), all the reported contacts in Tables 3 and 4 showed the expected BP joining the atoms involved, with their corresponding BCP in between (Fig. 5). The values obtained for the density and Laplacian (in the two rightmost columns of these Tables) correlate with corresponding values in similar analyses in the literature (Steiner, 2002; Novoa & Mota, 2000; Di Paolo *et al.*, 2016). As expected for attractive closed-shell interactions (Bader & Essén, 1984), the values obtained for $G(r)$ are (slightly) larger than those for $V(r)$, with $E(r)$ being positive and close to zero.

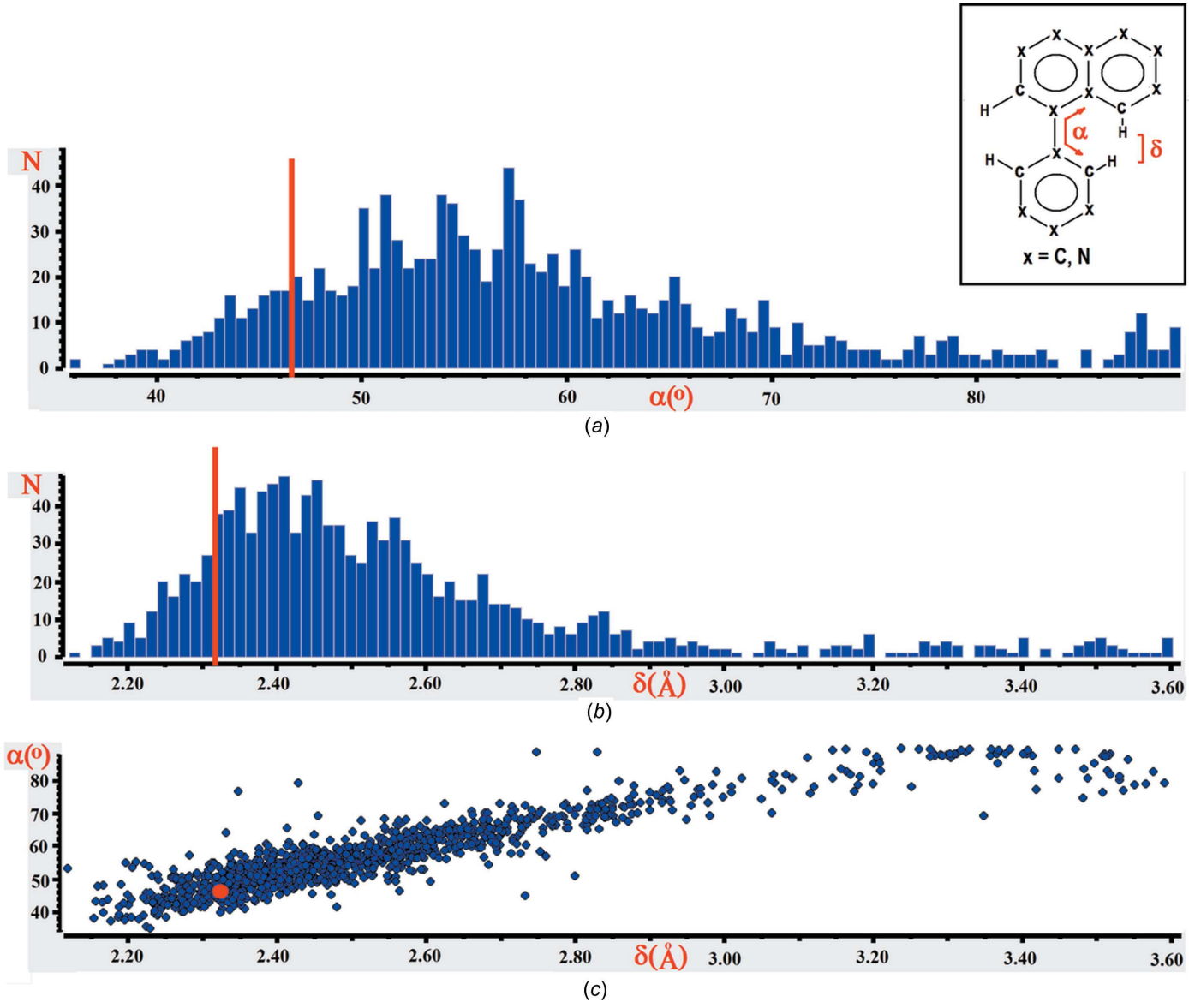


**Figure 3**
Statistical data for $\alpha$ and $\delta$ (as defined in the inset) from ≃1100 cases in the CSD (Version 5.37; Groom *et al.*, 2016), showing (*a*) a histogram of the dihedral angle $\alpha$, (*b*) a histogram of the H···H distance $\delta$ and (*c*) a scatterplot of both.

**Table 4**
$\pi$–$\pi$ contacts.

The ring codes are defined in Fig. 1. Notes: ccd is the centre-to-centre distance, da is the dihedral angle between rings, sa is the slippage angle and ipd is the interplanar distance or the (mean) distance from one plane to the neighbouring centroid. For details, see Janiak (2000).

| Interaction code | $Cg\cdots Cg$ | ccd (Å) | da (°) | sa (°) | ipd (Å) | $100\rho(r)$ (a.u) | $100\nabla^2\rho(r)$(a.u) |
|---|---|---|---|---|---|---|---|
| #3 | $Cg2\cdots Cg1^{iii}$ | 3.7750 (8) | 7.90 (7) | 22.2 (18) | 3.48 (5) | 0.52 | 0.15 |
| #4 | $Cg3\cdots Cg2^{iii}$ | 3.7700 (8) | 2.24 (7) | 26.1 (11) | 3.38 (3) | 0.55 | 0.16 |
| #5 | $Cg4\cdots Cg5^{iv}$ | 4.1539 (9) | 11.43 (8) | 29 (5) | 3.6 (2) | 0.30 | 0.10 |

Symmetry codes: (iii) $-x+1, -y+1, -z$; (iv) $-x+\frac{1}{2}, y-\frac{1}{2}, -z+\frac{1}{2}$.

So, in this first step, our AIM calculations confirmed the bonding character of all the noncovalent interactions reported in Tables 3 and 4. But besides its capacity of confirming what is obvious from other methods, we were looking in AIM for the ability to cast light where other methods had failed, in order to justify its inclusion in our personal panoply of crystallographic tools.

In this respect, the present structure provides some modest, though illuminating, contributions. The first is given by C—H···N contact #1* in Table 3, which, even if similar in nature to the un-objectionable #1, presents borderline N···H and C—H···N parameters, so that it is considered in contradictory ways by well established structure analysis software (as used with their standard settings), *viz.* the contact was ignored as a genuine hydrogen bond by *PLATON* (Spek, 2009), but ascribed a genuine bonding character by *Mercury* (Macrae *et al.*, 2006). When analyzed through the AIM procedure, a bond path was found joining atoms H13 and N1$^{ii}$ [symmetry code: (ii) $x-\frac{1}{2}, -y+\frac{1}{2}, z-\frac{1}{2}$], and the calculated parameters of $100\rho(r)$ = 0.80 a.u. and $100\nabla^2\rho(r)$ = 0.24 a.u (a.u. = atomic units) give account of a weak, though not negligible, interaction.

An especially interesting case was that of the tpy–isq dihedral angle [$\alpha$ = 46.57 (6)°] and its associated C7—H7···H23—C23 contact ($\delta$ = 2.32 Å) discussed above. An optimization of the X-ray molecular model, having $\alpha$ as the free variable with a wide range of starting values ($\alpha$ = 10 to 80°) systematically converged to a common final result, with $\alpha$ = 48 (1)°, within error limits identical to the experimental value and suggesting this as a favoured equilibrium position. Concomitantly, a clear BP appears joining atoms H7 and H23 (Figs. 1 and 5), with a BCP roughly midway. The calculated values $100\rho(r)$ = 1.18 a.u. and $100\nabla^2\rho(r)$ = 0.43 a.u. give this interaction a similar character to, for example, #1 in Table 3.

In contrast with the above 'confirmations', in the case of the short intramolecular C—H···N contacts involving the py group of the tpy core, AIM calculations disclosed no bond paths joining the H···N pairs. Thus, and against our own previous expectations, nonbonding interactions seems to link these atom pairs.

However, molecular optimization with freely rotating py groups provided quite interesting results. Having the $\varphi$ rotation angle around the C—C bond as the minimization variable, the starting point from $\varphi = 0°$ (corresponding to a planar tpy

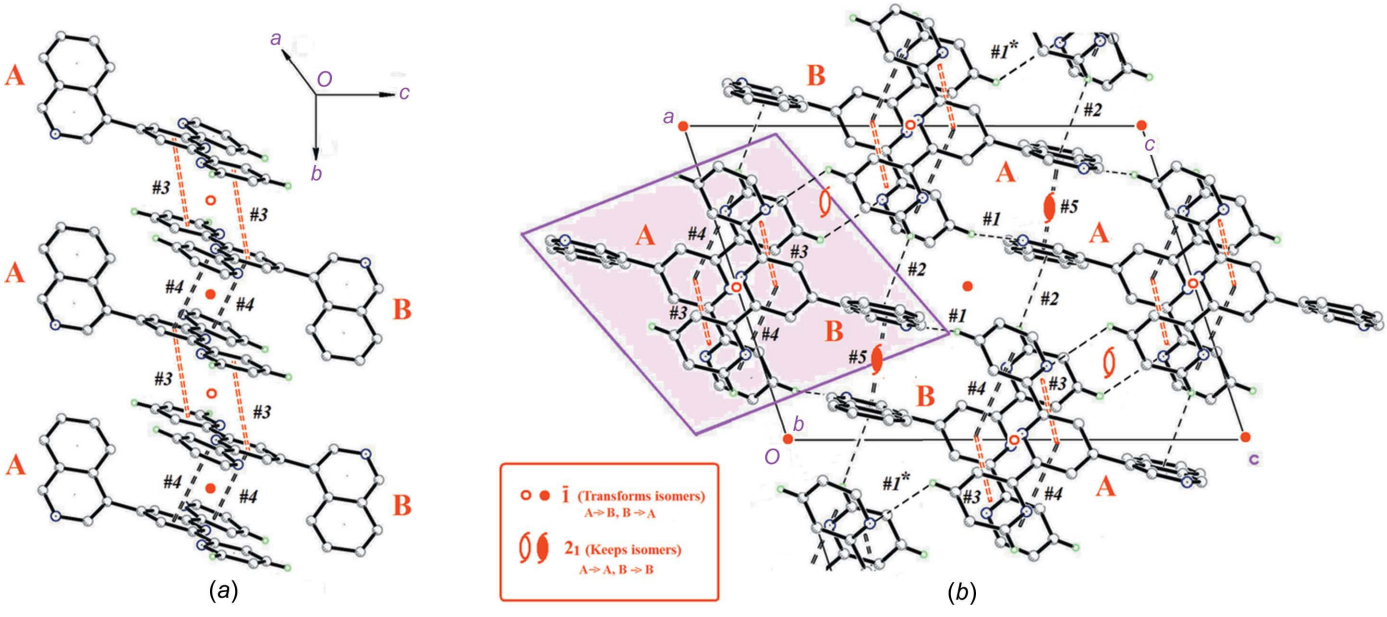


**Figure 4**
Packing views of (I), showing (*a*) the formation of a single column along [010], (*b*) an assembly of columns into a three-dimensional supramolecular structure. The highlighted area shows one single column seen in projection. C—H···N/$\pi$ interactions are shown with plain broken lines and $\pi$–$\pi$ interactions are shown with double broken lines (#*n* reference codes as defined in Tables 3 and 4).

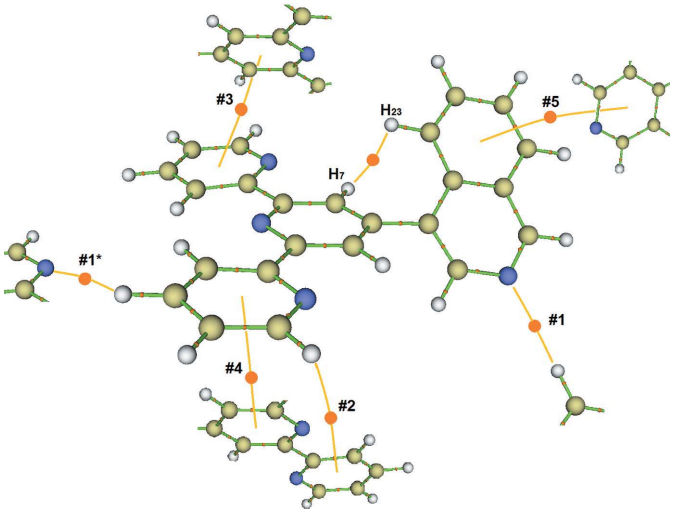


**Figure 5**
Bond paths and critical points in (I). See Tables 3 and 4 for definitions of the interaction codes.

with the N atoms in *cis* positions) ended up in a $\varphi = 25^\circ$ final angle, exemplifying the disruptive effect of the repulsion of the free pairs at $\varphi = 0^\circ$, and confirming that the planar 'triple-bite' situation in coordination complexes is only sustainable with strong binding forces to the metal atom. On the other hand, when starting at $\varphi = 90^\circ$ (lateral py groups at right angles to the central core), the minimization process clearly drove it to the experimental equilibrium position $\varphi \simeq 180^\circ$, suggesting that even if not clamped by intramolecular N···H bonds (according to our AIM results), this planar set-up is anyway a stable energy minimum.

## 4. Summary

We gained confidence about the usefulness of AIM as a complementary crystallographic tool, expanding the reach of the usual techniques. Through its use, in addition to confirming the findings made through conventional methods of analysis, we have been able to provide certainties where the latter had little or nothing to say. In other words, the present results make clear that a cautious use of AIM can help in the clarification of borderline cases, when the bare geometrical arguments would not suffice. We shall strive in applying the technique whenever appropriate.

## Acknowledgements

The authors acknowledge Universidad de La Frontera (Proyecto DIUFRO DI15-0027) and ANPCyT (project No. PME 2006-01113) for the purchase of the Oxford Gemini CCD diffractometer.

## References

Bader, R. F. W. (1990). In *Atoms in Molecules – a Quantum Theory*. Oxford University Press.
Bader, R. F. W. (2009). *J. Phys. Chem. A*, **113**, 10391–10396.
Bader, R. F. W. & Essén, H. (1984). *J. Chem. Phys.* **80**, 1943–1960.
Constable, E. C. (2007). *Chem. Soc. Rev.* **36**, 246–253.
Di Paolo, M., Bossi, M. L., Baggio, R. & Suarez, S. A. (2016). *Acta Cryst.* B**72**, 684–692.
Dunitz, J. D. (2015). *IUCrJ*, **2**, 157–158.
Eryazici, I., Moorefield, Ch. N. & Newkome, G. R. (2008). *Chem. Rev.* **108**, 1834–1895.
Frisch, M. J., *et al.* (2009). *GAUSSIAN09*. Gaussian Inc., Wallingford, Connecticut, USA. http://www.gaussian.com
Groom, C. R., Bruno, I. J., Lightfoot, M. P. & Ward, S. C. (2016). *Acta Cryst.* B**72**, 171–179.
Gulyani, A. R., Srinivasa Gopalan, R., Kulkarni, G. U. & Bhattacharya, S. (2002). *J. Mol. Struct.* **616**, 103–112.
Haaland, A., Shorokhov, D. J. & Tverdova, N. V. (2004). *Chem. Eur. J.* **10**, 4416–4421.
Hanan, G. R. & Wang, J. (2005). *Synlett*, **8**, 1251–1254.
Janiak, C. (2000). *J. Chem. Soc. Dalton Trans.* pp. 3885–3898.
Krapp, A. & Frenking, G. (2007). *Chem. Eur. J.* **13**, 8256–8270.
Lecomte, C., Espinosa, E. & Matta, C. F. (2015). *IUCrJ*, **2**, 161–163.
Lu, T. & Chen, F. (2012). *J. Comput. Chem.* **33**, 580–592.
Macrae, C. F., Edgington, P. R., McCabe, P., Pidcock, E., Shields, G. P., Taylor, R., Towler, M. & van de Streek, J. (2006). *J. Appl. Cryst.* **39**, 453–457.
Novoa, J. J. & Mota, S. (2000). *Chem. Phys. Lett.* **318**, 345–354.
Oxford Diffraction (2009). *CrysAlis PRO*. Oxford Diffraction Ltd, Yarnton, Oxfordshire, England.
Poater, J., Solá, M. & Bickelhaupt, F. M. (2006). *Chem. Eur. J.* **12**, 2902–2905.
Sheldrick, G. M. (2008). *Acta Cryst.* A**64**, 112–122.
Sheldrick, G. M. (2015). *Acta Cryst.* C**71**, 3–8.
Spackman, M. (2015). *Cryst. Growth Des.* **15**, 5624–5628.
Spek, A. L. (2009). *Acta Cryst.* D**65**, 148–155.
Steiner, T. (2002). *Angew. Chem. Int. Ed.* **41**, 48–76.
Thakur, T. S., Dubey, R. & Desiraju, G. R. (2015). *IUCrJ*, **2**, 159–160.
Wang, G., Chen, Z., Xu, Z., Wang, J., Yang, Y., Cai, T., Shi, J. & Zhu, W. (2016). *J. Phys. Chem. B*, **120**, 610–620.

# supporting information

*Acta Cryst.* (2016). C**72**, 932-938 [https://doi.org/10.1107/S2053229616016533]

## Structural and theoretical characterization of a new twisted 4′-substituted terpyridine compound: 4′-(isoquinolin-4-yl)-2,2′:6′,2′′-terpyridine

**Juan Granifo, Beatriz Arévalo, Rubén Gaviño, Sebastián Suárez and Ricardo Baggio**

### Computing details

Data collection: *CrysAlis PRO* (Oxford Diffraction, 2009); cell refinement: *CrysAlis PRO* (Oxford Diffraction, 2009); data reduction: *CrysAlis PRO* (Oxford Diffraction, 2009); program(s) used to solve structure: *SHELXS97* (Sheldrick, 2008); program(s) used to refine structure: *SHELXL2014* (Sheldrick, 2015); molecular graphics: *SHELXTL* (Sheldrick, 2008) and *Mercury* (Macrae *et al.*, 2006); software used to prepare material for publication: *SHELXL2014* (Sheldrick, 2015) and *PLATON* (Spek, 2009).

### 4′-(Isoquinolin-4-yl)-2,2′:6′,2′′-terpyridine

*Crystal data*

$C_{24}H_{16}N_4$
$M_r = 360.41$
Monoclinic, $P2_1/n$
$a = 12.3897$ (3) Å
$b = 8.7940$ (3) Å
$c = 17.1791$ (6) Å
$\beta = 108.369$ (3)°
$V = 1776.38$ (10) Å$^3$
$Z = 4$
$F(000) = 752$
$D_x = 1.348$ Mg m$^{-3}$
Mo $K\alpha$ radiation, $\lambda = 0.71073$ Å
Cell parameters from 6249 reflections
$\theta = 3.9$–$27.7°$
$\mu = 0.08$ mm$^{-1}$
$T = 170$ K
Prism, colourless
0.34 × 0.22 × 0.12 mm

*Data collection*

Oxford Diffraction Xcalibur CCD (Eos, Gemini) diffractometer
Graphite monochromator
$\omega$ scans
Absorption correction: multi-scan (CrysAlis PRO; Oxford Diffraction, 2009)
$T_{min} = 0.97$, $T_{max} = 1.00$
18351 measured reflections
4225 independent reflections
3138 reflections with $I > 2\sigma(I)$
$R_{int} = 0.038$
$\theta_{max} = 28.9°$, $\theta_{min} = 3.6°$
$h = -16 \rightarrow 16$
$k = -9 \rightarrow 11$
$l = -22 \rightarrow 23$

*Refinement*

Refinement on $F^2$
Least-squares matrix: full
$R[F^2 > 2\sigma(F^2)] = 0.044$
$wR(F^2) = 0.123$
$S = 1.02$
4225 reflections
254 parameters
0 restraints
Hydrogen site location: inferred from neighbouring sites
H-atom parameters constrained
$w = 1/[\sigma^2(F_o^2) + (0.0527P)^2 + 0.4471P]$ where $P = (F_o^2 + 2F_c^2)/3$
$(\Delta/\sigma)_{max} < 0.001$
$\Delta\rho_{max} = 0.26$ e Å$^{-3}$
$\Delta\rho_{min} = -0.20$ e Å$^{-3}$

Extinction correction: SHELXL2014 (Sheldrick, 2015), $Fc^*=kFc[1+0.001xFc^2\lambda^3/\sin(2\theta)]^{-1/4}$
Extinction coefficient: 0.0124 (13)

*Special details*

**Geometry**. All e.s.d.'s (except the e.s.d. in the dihedral angle between two l.s. planes) are estimated using the full covariance matrix. The cell e.s.d.'s are taken into account individually in the estimation of e.s.d.'s in distances, angles and torsion angles; correlations between e.s.d.'s in cell parameters are only used when they are defined by crystal symmetry. An approximate (isotropic) treatment of cell e.s.d.'s is used for estimating e.s.d.'s involving l.s. planes.

*Fractional atomic coordinates and isotropic or equivalent isotropic displacement parameters (Å²)*

| | *x* | *y* | *z* | $U_{iso}$*/$U_{eq}$ |
|---|---|---|---|---|
| N1 | 0.73444 (9) | 0.54800 (14) | 0.11880 (7) | 0.0274 (3) |
| N2 | 0.51893 (9) | 0.27644 (13) | 0.01691 (7) | 0.0237 (3) |
| N3 | 0.27126 (10) | 0.03477 (14) | −0.03023 (7) | 0.0296 (3) |
| N4 | 0.36475 (11) | 0.24792 (17) | 0.34177 (8) | 0.0412 (4) |
| C1 | 0.82661 (12) | 0.61388 (17) | 0.10901 (9) | 0.0308 (3) |
| H1 | 0.8632 | 0.6888 | 0.1462 | 0.037* |
| C2 | 0.87058 (12) | 0.57697 (17) | 0.04677 (9) | 0.0319 (3) |
| H2 | 0.9351 | 0.6257 | 0.0424 | 0.038* |
| C3 | 0.81662 (12) | 0.46642 (17) | −0.00855 (9) | 0.0324 (3) |
| H3 | 0.8442 | 0.4389 | −0.0510 | 0.039* |
| C4 | 0.72084 (12) | 0.39693 (16) | −0.00006 (9) | 0.0273 (3) |
| H4 | 0.6830 | 0.3220 | −0.0367 | 0.033* |
| C5 | 0.68206 (10) | 0.44116 (15) | 0.06438 (8) | 0.0221 (3) |
| C6 | 0.57955 (10) | 0.36965 (15) | 0.07620 (8) | 0.0224 (3) |
| C7 | 0.55043 (11) | 0.39990 (15) | 0.14679 (8) | 0.0238 (3) |
| H7 | 0.5952 | 0.4644 | 0.1870 | 0.029* |
| C8 | 0.45389 (11) | 0.33261 (16) | 0.15643 (8) | 0.0244 (3) |
| C9 | 0.39205 (11) | 0.23408 (15) | 0.09548 (8) | 0.0247 (3) |
| H9 | 0.3279 | 0.1854 | 0.1004 | 0.030* |
| C10 | 0.42695 (10) | 0.20867 (15) | 0.02681 (8) | 0.0231 (3) |
| C11 | 0.36231 (11) | 0.10557 (15) | −0.04007 (8) | 0.0241 (3) |
| C12 | 0.39502 (12) | 0.08606 (17) | −0.10971 (9) | 0.0305 (3) |
| H12 | 0.4582 | 0.1370 | −0.1148 | 0.037* |
| C13 | 0.33292 (14) | −0.00957 (18) | −0.17121 (9) | 0.0363 (4) |
| H13 | 0.3535 | −0.0240 | −0.2183 | 0.044* |
| C14 | 0.23981 (13) | −0.08322 (18) | −0.16149 (9) | 0.0344 (4) |
| H14 | 0.1965 | −0.1489 | −0.2016 | 0.041* |
| C15 | 0.21250 (12) | −0.05715 (17) | −0.09083 (10) | 0.0338 (3) |
| H15 | 0.1492 | −0.1066 | −0.0849 | 0.041* |
| C16 | 0.41990 (11) | 0.36066 (16) | 0.23095 (8) | 0.0250 (3) |
| C17 | 0.39188 (12) | 0.23932 (18) | 0.27095 (9) | 0.0326 (3) |
| H17 | 0.3914 | 0.1435 | 0.2479 | 0.039* |
| C18 | 0.36569 (13) | 0.3839 (2) | 0.37317 (10) | 0.0412 (4) |
| H18 | 0.3484 | 0.3917 | 0.4219 | 0.049* |
| C19 | 0.39101 (11) | 0.51904 (19) | 0.33848 (9) | 0.0344 (4) |

| | | | | |
|---|---|---|---|---|
| C20 | 0.39052 (13) | 0.6628 (2) | 0.37540 (11) | 0.0473 (5) |
| H20 | 0.3746 | 0.6693 | 0.4247 | 0.057* |
| C21 | 0.41314 (15) | 0.7914 (2) | 0.33940 (13) | 0.0550 (5) |
| H21 | 0.4132 | 0.8854 | 0.3643 | 0.066* |
| C22 | 0.43630 (14) | 0.7822 (2) | 0.26487 (12) | 0.0469 (5) |
| H22 | 0.4506 | 0.8709 | 0.2403 | 0.056* |
| C23 | 0.43836 (12) | 0.64552 (17) | 0.22752 (10) | 0.0335 (3) |
| H23 | 0.4534 | 0.6423 | 0.1778 | 0.040* |
| C24 | 0.41772 (11) | 0.50872 (17) | 0.26402 (9) | 0.0277 (3) |

*Atomic displacement parameters (Å²)*

| | $U^{11}$ | $U^{22}$ | $U^{33}$ | $U^{12}$ | $U^{13}$ | $U^{23}$ |
|---|---|---|---|---|---|---|
| N1 | 0.0266 (6) | 0.0296 (7) | 0.0254 (6) | −0.0031 (5) | 0.0073 (5) | −0.0006 (5) |
| N2 | 0.0244 (5) | 0.0236 (6) | 0.0231 (6) | 0.0003 (4) | 0.0077 (5) | 0.0011 (5) |
| N3 | 0.0265 (6) | 0.0282 (7) | 0.0328 (7) | −0.0027 (5) | 0.0074 (5) | −0.0008 (5) |
| N4 | 0.0406 (7) | 0.0548 (9) | 0.0337 (8) | 0.0024 (6) | 0.0197 (6) | 0.0091 (7) |
| C1 | 0.0277 (7) | 0.0324 (8) | 0.0300 (8) | −0.0057 (6) | 0.0056 (6) | 0.0008 (6) |
| C2 | 0.0240 (7) | 0.0357 (8) | 0.0372 (8) | −0.0016 (6) | 0.0114 (6) | 0.0093 (7) |
| C3 | 0.0331 (7) | 0.0365 (9) | 0.0324 (8) | 0.0029 (6) | 0.0171 (6) | 0.0050 (7) |
| C4 | 0.0296 (7) | 0.0280 (7) | 0.0256 (7) | 0.0003 (6) | 0.0108 (6) | 0.0004 (6) |
| C5 | 0.0225 (6) | 0.0221 (7) | 0.0211 (7) | 0.0014 (5) | 0.0059 (5) | 0.0033 (5) |
| C6 | 0.0224 (6) | 0.0215 (7) | 0.0230 (7) | 0.0025 (5) | 0.0065 (5) | 0.0018 (5) |
| C7 | 0.0244 (6) | 0.0236 (7) | 0.0237 (7) | −0.0001 (5) | 0.0079 (5) | −0.0030 (5) |
| C8 | 0.0240 (6) | 0.0248 (7) | 0.0252 (7) | 0.0038 (5) | 0.0089 (5) | 0.0012 (6) |
| C9 | 0.0229 (6) | 0.0254 (7) | 0.0274 (7) | 0.0005 (5) | 0.0104 (5) | 0.0015 (6) |
| C10 | 0.0229 (6) | 0.0218 (7) | 0.0237 (7) | 0.0024 (5) | 0.0059 (5) | 0.0016 (5) |
| C11 | 0.0247 (6) | 0.0203 (7) | 0.0251 (7) | 0.0023 (5) | 0.0050 (5) | 0.0026 (5) |
| C12 | 0.0339 (7) | 0.0312 (8) | 0.0252 (7) | −0.0035 (6) | 0.0078 (6) | −0.0014 (6) |
| C13 | 0.0456 (9) | 0.0366 (9) | 0.0241 (8) | 0.0000 (7) | 0.0072 (6) | −0.0034 (7) |
| C14 | 0.0361 (8) | 0.0286 (8) | 0.0286 (8) | −0.0002 (6) | −0.0039 (6) | −0.0021 (6) |
| C15 | 0.0274 (7) | 0.0291 (8) | 0.0390 (9) | −0.0022 (6) | 0.0020 (6) | 0.0003 (7) |
| C16 | 0.0209 (6) | 0.0311 (8) | 0.0235 (7) | 0.0017 (5) | 0.0076 (5) | −0.0017 (6) |
| C17 | 0.0328 (7) | 0.0360 (9) | 0.0322 (8) | 0.0024 (6) | 0.0149 (6) | 0.0045 (7) |
| C18 | 0.0349 (8) | 0.0669 (12) | 0.0260 (8) | 0.0018 (8) | 0.0158 (7) | −0.0007 (8) |
| C19 | 0.0220 (7) | 0.0529 (10) | 0.0298 (8) | −0.0003 (6) | 0.0105 (6) | −0.0108 (7) |
| C20 | 0.0297 (8) | 0.0707 (13) | 0.0457 (10) | −0.0051 (8) | 0.0182 (7) | −0.0284 (9) |
| C21 | 0.0431 (9) | 0.0526 (12) | 0.0773 (14) | −0.0085 (8) | 0.0302 (10) | −0.0377 (11) |
| C22 | 0.0444 (9) | 0.0365 (9) | 0.0677 (12) | −0.0018 (7) | 0.0287 (9) | −0.0128 (9) |
| C23 | 0.0305 (7) | 0.0330 (8) | 0.0406 (9) | 0.0007 (6) | 0.0164 (7) | −0.0066 (7) |
| C24 | 0.0193 (6) | 0.0367 (8) | 0.0280 (7) | 0.0011 (6) | 0.0086 (5) | −0.0049 (6) |

*Geometric parameters (Å, º)*

| | | | |
|---|---|---|---|
| N1—C1 | 1.3376 (17) | C10—C11 | 1.4845 (19) |
| N1—C5 | 1.3400 (17) | C11—C12 | 1.3894 (19) |
| N2—C6 | 1.3384 (17) | C12—C13 | 1.380 (2) |
| N2—C10 | 1.3435 (16) | C12—H12 | 0.9300 |

| | | | |
|---|---|---|---|
| N3—C15 | 1.3377 (19) | C13—C14 | 1.378 (2) |
| N3—C11 | 1.3450 (17) | C13—H13 | 0.9300 |
| N4—C18 | 1.310 (2) | C14—C15 | 1.378 (2) |
| N4—C17 | 1.3626 (18) | C14—H14 | 0.9300 |
| C1—C2 | 1.383 (2) | C15—H15 | 0.9300 |
| C1—H1 | 0.9300 | C16—C17 | 1.372 (2) |
| C2—C3 | 1.377 (2) | C16—C24 | 1.4243 (19) |
| C2—H2 | 0.9300 | C17—H17 | 0.9300 |
| C3—C4 | 1.3829 (19) | C18—C19 | 1.409 (2) |
| C3—H3 | 0.9300 | C18—H18 | 0.9300 |
| C4—C5 | 1.3938 (18) | C19—C20 | 1.415 (2) |
| C4—H4 | 0.9300 | C19—C24 | 1.4216 (19) |
| C5—C6 | 1.4873 (17) | C20—C21 | 1.360 (3) |
| C6—C7 | 1.3955 (18) | C20—H20 | 0.9300 |
| C7—C8 | 1.3903 (18) | C21—C22 | 1.400 (3) |
| C7—H7 | 0.9300 | C21—H21 | 0.9300 |
| C8—C9 | 1.3887 (19) | C22—C23 | 1.366 (2) |
| C8—C16 | 1.4888 (18) | C22—H22 | 0.9300 |
| C9—C10 | 1.3965 (18) | C23—C24 | 1.417 (2) |
| C9—H9 | 0.9300 | C23—H23 | 0.9300 |

| | | | |
|---|---|---|---|
| C1—N1—C5 | 117.44 (12) | C13—C12—H12 | 120.3 |
| C6—N2—C10 | 118.06 (11) | C11—C12—H12 | 120.3 |
| C15—N3—C11 | 117.01 (12) | C14—C13—C12 | 118.68 (14) |
| C18—N4—C17 | 116.46 (14) | C14—C13—H13 | 120.7 |
| N1—C1—C2 | 123.75 (14) | C12—C13—H13 | 120.7 |
| N1—C1—H1 | 118.1 | C15—C14—C13 | 118.40 (14) |
| C2—C1—H1 | 118.1 | C15—C14—H14 | 120.8 |
| C3—C2—C1 | 118.40 (13) | C13—C14—H14 | 120.8 |
| C3—C2—H2 | 120.8 | N3—C15—C14 | 124.16 (14) |
| C1—C2—H2 | 120.8 | N3—C15—H15 | 117.9 |
| C2—C3—C4 | 119.05 (13) | C14—C15—H15 | 117.9 |
| C2—C3—H3 | 120.5 | C17—C16—C24 | 118.15 (13) |
| C4—C3—H3 | 120.5 | C17—C16—C8 | 119.12 (13) |
| C3—C4—C5 | 118.85 (13) | C24—C16—C8 | 122.72 (12) |
| C3—C4—H4 | 120.6 | N4—C17—C16 | 125.22 (15) |
| C5—C4—H4 | 120.6 | N4—C17—H17 | 117.4 |
| N1—C5—C4 | 122.51 (12) | C16—C17—H17 | 117.4 |
| N1—C5—C6 | 116.60 (11) | N4—C18—C19 | 124.76 (14) |
| C4—C5—C6 | 120.89 (12) | N4—C18—H18 | 117.6 |
| N2—C6—C7 | 122.77 (12) | C19—C18—H18 | 117.6 |
| N2—C6—C5 | 116.97 (11) | C18—C19—C20 | 122.09 (15) |
| C7—C6—C5 | 120.25 (12) | C18—C19—C24 | 118.22 (14) |
| C8—C7—C6 | 119.35 (12) | C20—C19—C24 | 119.70 (15) |
| C8—C7—H7 | 120.3 | C21—C20—C19 | 120.57 (15) |
| C6—C7—H7 | 120.3 | C21—C20—H20 | 119.7 |
| C9—C8—C7 | 117.82 (12) | C19—C20—H20 | 119.7 |
| C9—C8—C16 | 120.88 (12) | C20—C21—C22 | 119.91 (16) |

| | | | |
|---|---|---|---|
| C7—C8—C16 | 121.26 (12) | C20—C21—H21 | 120.0 |
| C8—C9—C10 | 119.51 (12) | C22—C21—H21 | 120.0 |
| C8—C9—H9 | 120.2 | C23—C22—C21 | 121.34 (17) |
| C10—C9—H9 | 120.2 | C23—C22—H22 | 119.3 |
| N2—C10—C9 | 122.47 (12) | C21—C22—H22 | 119.3 |
| N2—C10—C11 | 116.44 (11) | C22—C23—C24 | 120.42 (15) |
| C9—C10—C11 | 121.09 (12) | C22—C23—H23 | 119.8 |
| N3—C11—C12 | 122.34 (13) | C24—C23—H23 | 119.8 |
| N3—C11—C10 | 117.05 (12) | C23—C24—C19 | 118.02 (13) |
| C12—C11—C10 | 120.61 (12) | C23—C24—C16 | 124.82 (13) |
| C13—C12—C11 | 119.41 (14) | C19—C24—C16 | 117.15 (13) |